

Quantification Of Spatio-Temporal Changes In Soil Erosion Rates At Puttur Taluk, Dakshina Kannada District, Karnataka, India

Prasad Pujar^{1*}, Sowmya N J², Sandeep J Nayak³, Sanjay Shekhar N C⁴

DOI:10.47059/ml.v20i4.xyz

Abstract

Land degradation is one of the most severe and extensive environmental dangers the earth has been battling for a long time. Soil erosion is one of the prime factor for degradation of land as well as water resources. In this work, the amount of soil loss in the study region is calculated using the Revised Universal Soil Loss Equation (RUSLE) model and GIS.

The RUSLE model parameters are calculated using remote sensing data, and the erosion, probability zones are determined using GIS. Heavy rains in the year 2013 created flash floods over the region, resulting in the loss of 68,737 metric tonnes of soil. Very high erosion probability zone accounts for 61.3% of total soil loss (42,177 tons/year) and covers 6.69 percentage of the research area. The erosion susceptibility map that are produced as a result of this research would be a useful resource for stakeholders, decision-makers, and government officials involved in the planning and erosion catastrophe management.

Keywords: GIS, LU/LC, RUSLE, Soil Erosion.

INTRODUCTION

Recognizing the link between land use and management practices and soil quality change is crucial for the development of long-term land management strategies and actions. Degradation of land has been an issue for over a century, and it continues to be a major roadblock to long-term progress today. Soil erosion and water runoff are accountable for about 83% of the world's land degradation (Qian et al., 2015).

Numerous smallholders (farmers) employ low-cost ISWC techniques to reduce runoff and erosion. Soil property changes due to land usage must be evaluated in order to deal with issues of agroecosystem transformation and long-term land productivity. Human life depends on preventing soil and water loss and learning more about the soil erosion process and long-term growth specially in places like Puttur.

In the tropics, soil erosion poses a significant threat to agricultural sustainability, but it is a problem worldwide. When the pace of soil loss exceeds the rate at which topsoil is being replenished, soil productivity declines, and agricultural output and profits suffer.

Industrialization and urbanization convert forests and wetlands into farmland and human settlements. This shift in land use and land cover affects hydrological parameters such as soil erosion, sediment deposition in rivers and dams, and watershed stream flow. To measure the effects of natural vegetation changes on Earth's ecosystem, qualitative and quantitative Land use and Land cover (LU/LC) studies are needed.

If any research work where one wants to know how LU/LC changes over time and space, satellite images can be a great resource. Due to rising industrialization, urbanization, and

^{1*}Assistant Professor, Department of Civil Engineering, JSS Science and Technology University, Mysuru.

²Professor, Department of Civil Engineering, Vivekananda College of Engineering & Technology, Puttur.

³Professor, Department of Civil Engineering, Shree Madva Vadiraja Institute of Technology & Management, Bantakal, Udupi.

⁴Associate Professor, Department of Civil Engineering, JSS Academy of Technical Education Bengaluru.

forest-to-farmland conversions, land resources have been utilized to a larger level, resulting in land degradation (Ganasri and Ramesh 2016). The pattern of change in Land Use and Land Cover (LU/LC) is an important indicator of this shift. It is essential for planning and management purposes to have a thorough understanding of the patterns of land use and cover (Chauhan and Nayak 2005; Lin et al. 2009). Different economic and social systems occupying similar surroundings are an indication of the nature of a society's engagement with its physical environment, which is reflected in its land use patterns (Liu et al. 2009, Patel et al. 2019, Verburg et al. 2006). LU/LC shifts are a key concern in the context of global environmental change. Throughout history, many cultures have perished as a direct result of human abuse and overexploitation of the land as well as environmental interference (Hütt et al. 2016).

Vegetation cover is a key factor in decomposing precipitation into its aspects of hydrology such as surface runoff, base flow, groundwater flow, evapotranspiration, and so on. Consequently, watershed management and hydrological modelling depend largely on analysis of land use change trends (Wijesekara et al. 2012, Wang et al. 2021). Rapid shifts in both space and time characterise the process of land use change (Gumageri et al. 2011; Deviaet.al., 2015). It is widely acknowledged that the study of LU/LC change patterns and the assessment of their causes represents a trimming area of inquiry in the field of investigations of Natural Systems (Verburg et al. 1999, 2006; Niehoff et al. 2002; Patz, et al. 2005; Yuechen.2008;).

For the purpose of analysing and documenting spatial changes, the Geographic Information System (GIS) is an efficient instrument for handling secondary data.

Soil erosion is affected by the biophysical environment, which includes the soil, climate, terrain, ground cover, and their interactions. Soil erosion processes are affected by the slope, length, aspect, and shape of the landscape.

Runoff mechanism would be significantly impacted by slope and aspect. The steeper the slope, the more water runs off, and the less water soaks in. The slope's drainage finds a channel nearby, eroding the soil as its velocity increases. Steep slopes, climate (such as prolonged dry spells followed by high rainfall), poor land use, and land cover patterns are just few of the causes of soil erosion. Information about erosion rates, trends, and potential outcomes can be gleaned through well-executed models.

Soil erosion models come in a variety of sophistication levels. The Universal Soil Loss Equation (USLE), developed by Wischmeier and Smith in 1965, is a widely employed empirical model for assessing the rates of sheet and rill erosion. Considering that the original USLE was developed for usage in agricultural fields, Wischmeier and Smith (1959) presented a table for C factors that accounted for the crop type and growth stage. Differences in root structure and biomass among crops cause noticeable shifts in ground cover and, in turn, shifts in soil loss. The P factor is predicated on the assumption that different conservation methods will have different effects on soil depletion in a given agricultural setting.

To calculate annual average soil erosion using the USLE model, an empirical equation $A = RKLSCP$, can be employed (Wischmeier and Smith, 1978): Average annual soil erosion ($t\ ha^{-1}$), Rainfall erosivity ($MJ\ mm\ ha^{-1}\ h^{-1}$), and Soil Erodibility ($Mg\ h\ MJ^{-1}\ mm^{-1}$) are denoted by A, R, and K, respectively. L and S stand for the length and steepness of a slope, respectively, while C and P refer to crop management and conservation practises. In an RS GIS setting, one can determine the original crop component by computing the NDVI (Normalized Difference Vegetation Index), which measures the vitality of a plant's foliage. The C-factor is also based on the land use classification system in use there. In most cases, P factor is calculated using land use classification maps. From a DEM, one can easily determine the slope LS factor.

Soil erosion in croplands or on moderately sloping terrain was the original target of USLE's development. Erosion models are empirical, conceptual (partially empirical/mixed), and physically based. Soil erosion modelling requires DEMs, which can be built from analysing optical and microwave (SAR) remote sensing data (Borrelli et.al., 2021). When trying to determine the spatial pattern of soil loss across a large area, the RUSLE model's ability to estimate erosion potential on a cell-by-cell basis is invaluable. Isolating and querying these

areas in a GIS allows researchers to evaluate the importance of particular variables on erosion potential.

1. STUDY AREA

Fig. 1. shows the coordinates of Puttur the study area: 12.76480N 75.18240E. The average elevation is 87 metres (300 ft). The town of Puttur is located 32 miles (52 kilometres) South of Mangalore. There are 37 Panchayat villages spread across the study area of 4,559 km² (1,760 sq.m) in Puttur taluk. Puttur taluk has a tropical climate. It rains heavily for the most of the year. It is not as if the brief dry season is unimportant. The average annual temperature in Puttur is 26.8 degrees Celsius. On average, there are 4329 millimetres of precipitation per year. In the Puttur region, drought hits every year around the end of the year instead of the usual deluge. The hottest temperature ever recorded is 41.7 degrees Celsius, which occurred on March 5, 2013, at 3.15 p.m., in Putturhobli, which is located in the Puttur taluk of the Dakshina Kannada district. Thus, it is evident that the phenomenon of land use and land cover on soil conservation, and its relationship to climate changes, must be continuously monitored.

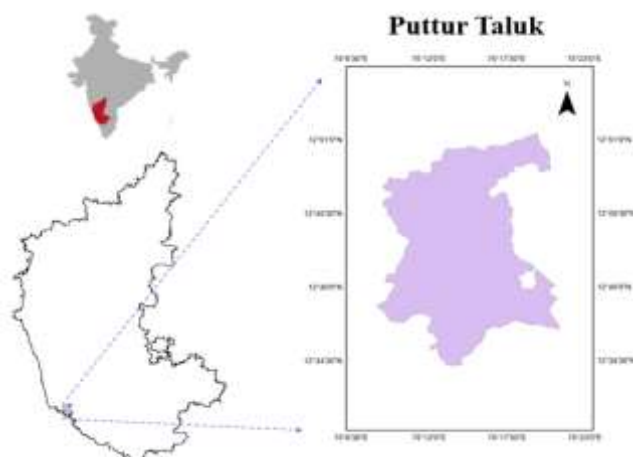


Fig 1: Location of the study area - Puttur Taluk

2. DATA

Satellite images from 1998, 2003, 2008, 2013, and 2019 supplied by the National Remote Sensing Center (NRSC) in Hyderabad (LISS-4, multispectral resolution of 5.8m) are used in the present study. IMD (India Meteorological Department) weather gauges record precipitation, temperature, humidity, wind speed, and daily sunshine are also collected for the present study.

3. Methodology and Parameter Estimation

Fig. 2. shows more detailed information about the methods used. By considering rainfall erosivity (R), cover management (C), slope length (LS), soil erodibility (K), and conservation practice parameters, the RUSLE model is used to determine annual soil loss patterns (P). In order to get an accurate reading, these factors must be adjusted for the level of erosion being measured. To reflect shifts in time, the RUSLE parameters must be determined in a categorical fashion.

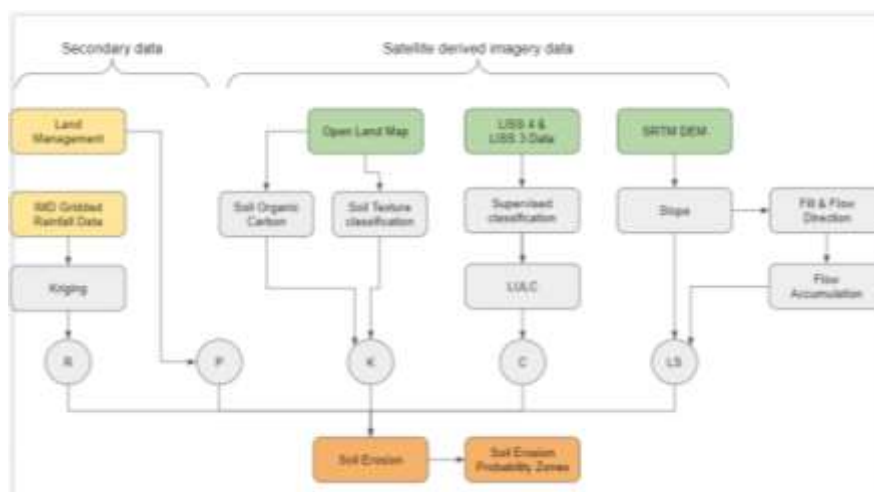


Fig 2: Methodology

3.1. Rainfall erosivity (R)

The rainfall erosivity factor quantifies rain's capacity to erode soil (R) and is given by the eq.(1). This erosivity factor is used by the RUSLE model to account for the interplay between the force exerted by falling raindrops, the length of time it takes for water to soak into the ground, and the rate at which it runs off the surface (R [$\text{MJ mm ha}^{-1} \text{h}^{-1} \text{yr}^{-1}$]).

$$\sum_1^{12} 1.735 \times 10^{(1.5 \log(\frac{P_1}{P}) - 0.8188)} \quad (1)$$

In the above equation, P1 is the average monthly rainfall, and P is the yearly rainfall. The annual precipitation in Puttur taluk is displayed in Figs. 3 to 7. Over the specified time period, annual precipitation in Puttur Taluk varied between 3200 and 4500 mm (1998-2019). The Ganasri et al. formula is used to determine rainfall erosivity (R) for the research area (2016). Figs. 8 to 12 illustrate the spatial distribution of R. Based on the 2013 erosivity map, R is determined by monthly precipitation patterns (Fig. 11).

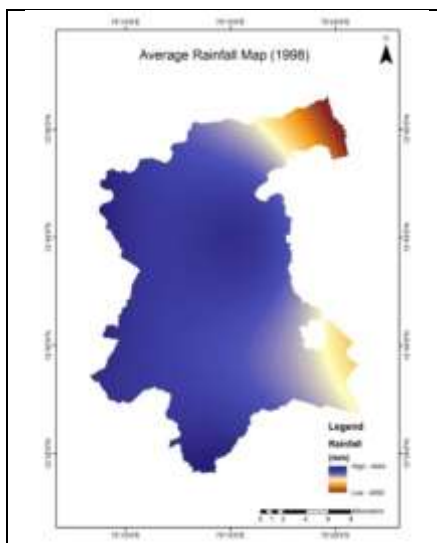


Fig 3: Annual rainfall map (1998)

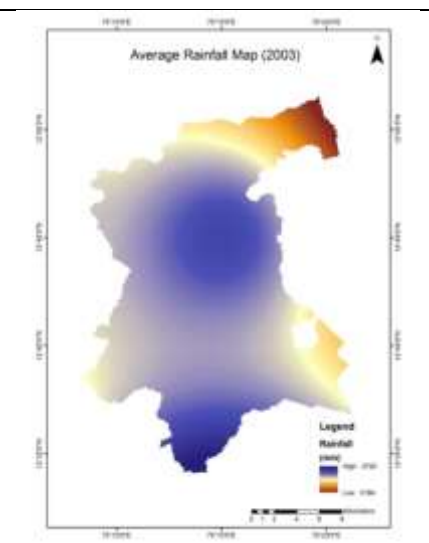


Fig 4: Annual rainfall map (2003)

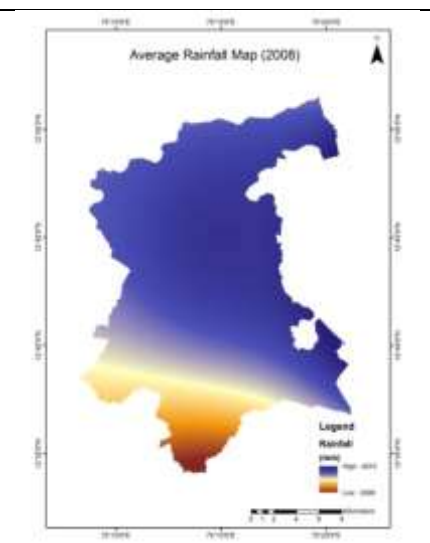


Fig 5: Annual rainfall map (2008)

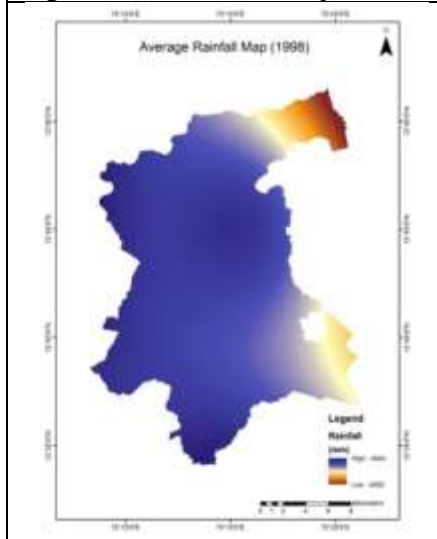


Fig 3: Annual rainfall map (1998)

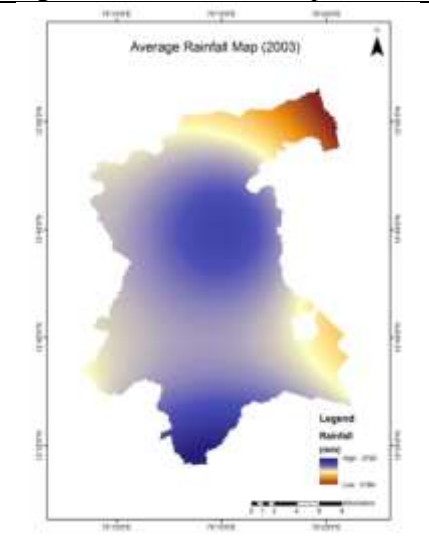


Fig 4: Annual rainfall map (2003)

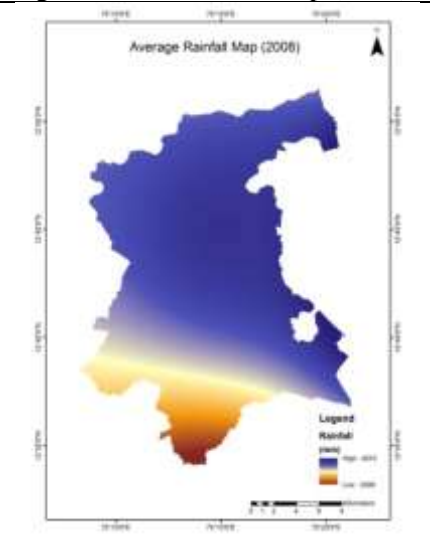


Fig 5: Annual rainfall map (2008)

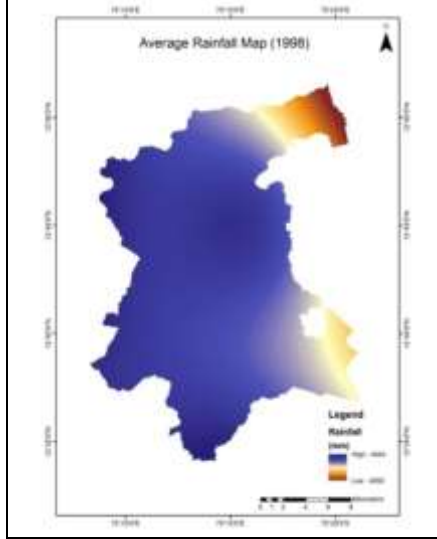


Fig 3: Annual rainfall map (1998)

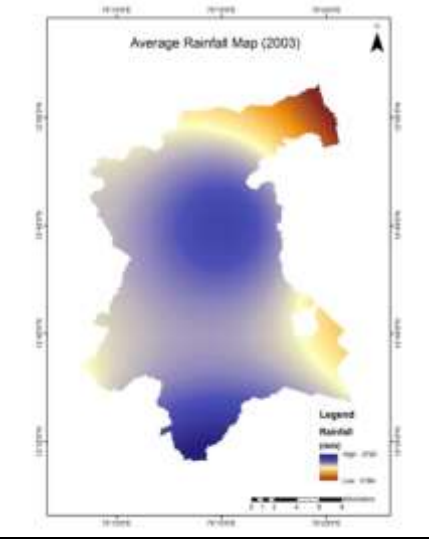


Fig 4: Annual rainfall map (2003)

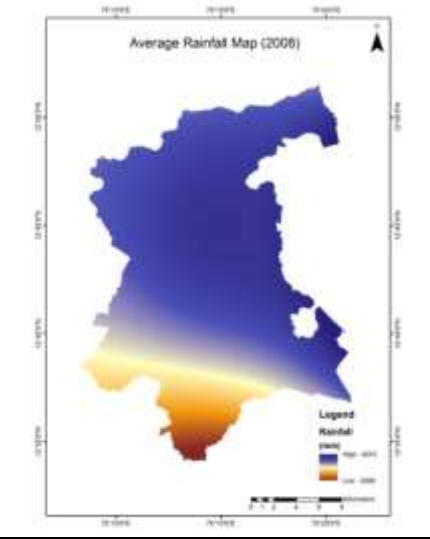


Fig 5: Annual rainfall map (2008)

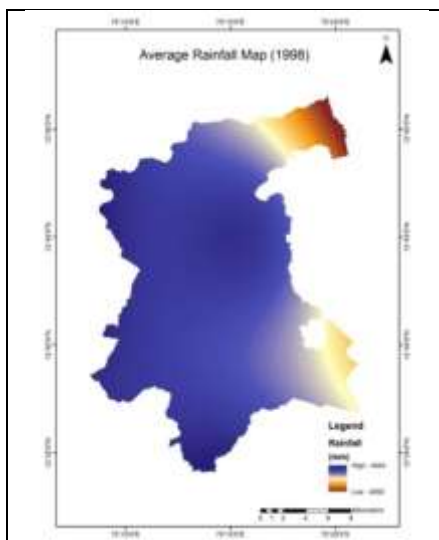


Fig 3: Annual rainfall map (1998)

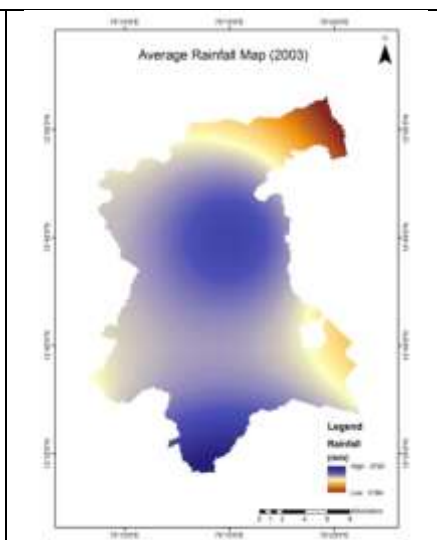


Fig 4: Annual rainfall map (2003)

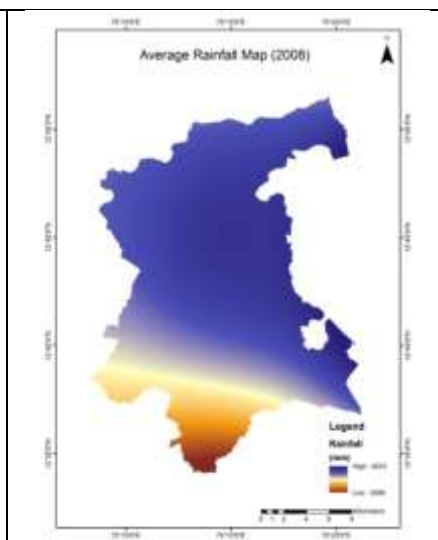


Fig 5: Annual rainfall map (2008)

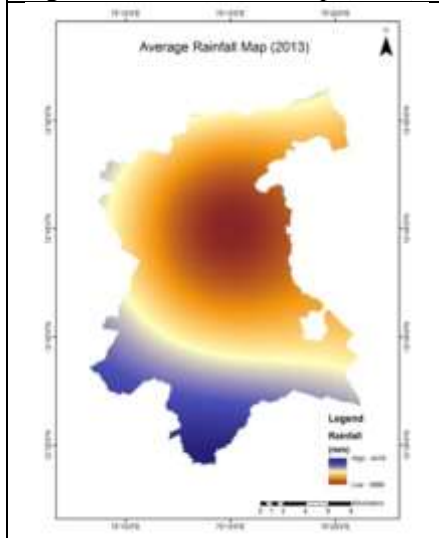


Fig 6: Annual rainfall map (2013)

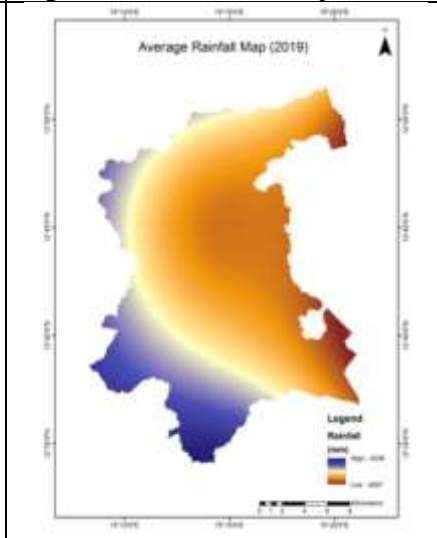


Fig 7: Annual rainfall map (2019)

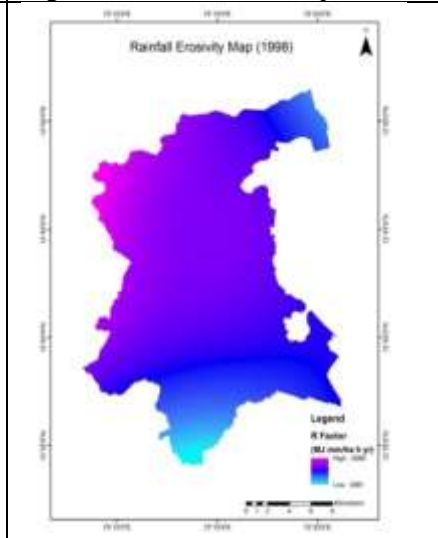


Fig 8: Rainfall erosivity map (1998)

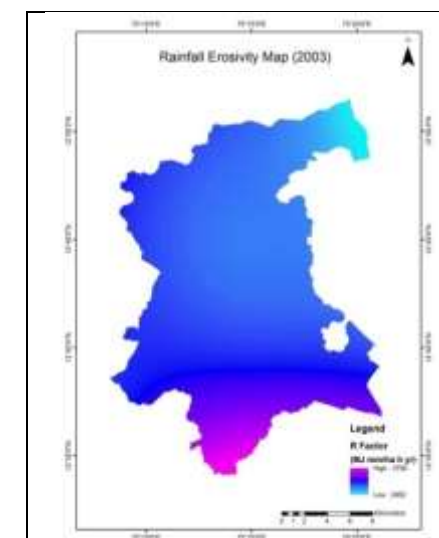


Fig 9: Rainfall erosivity map (2003)

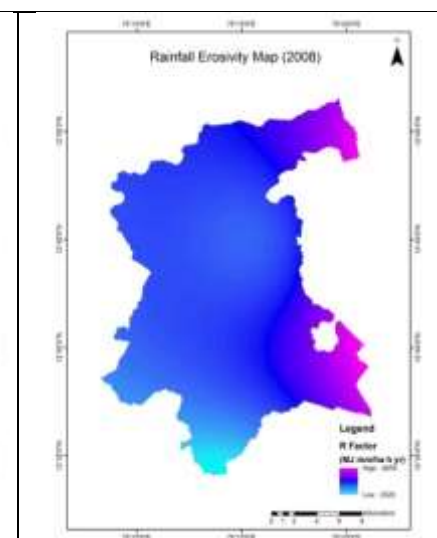


Fig 10: Rainfall erosivity map (2008)

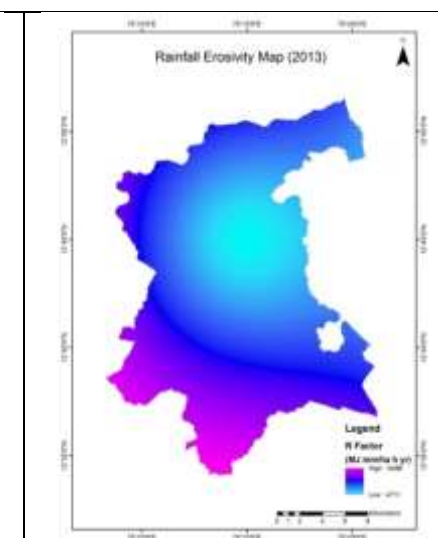


Fig 11: Rainfall erosivity map (2013)

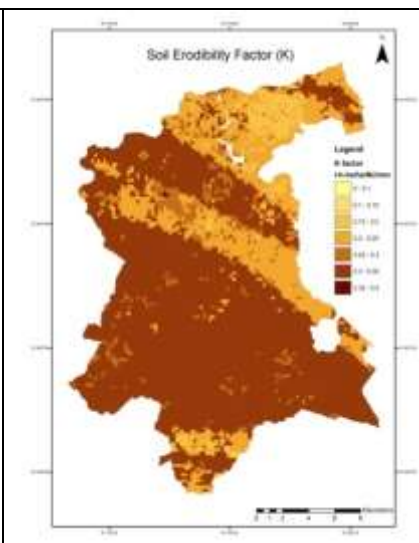
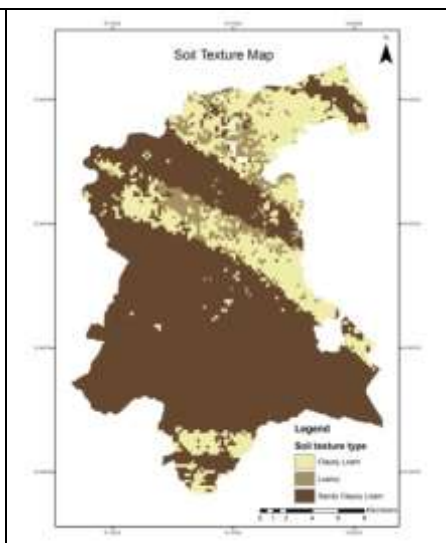
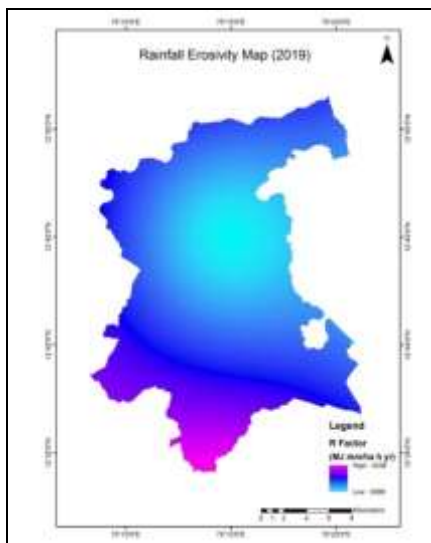


Fig 12: Rainfall erosivity map (2019)

Fig 13: Soil texture map

Fig 14: Soil erodibility factor

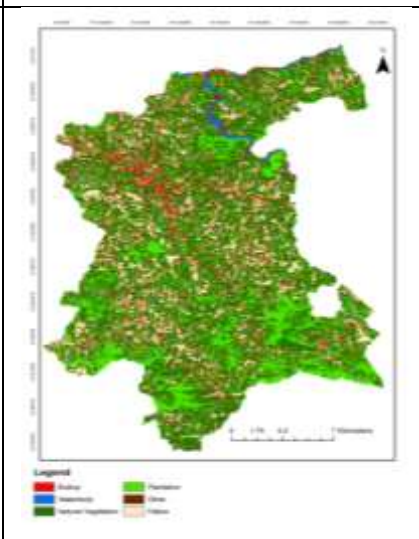
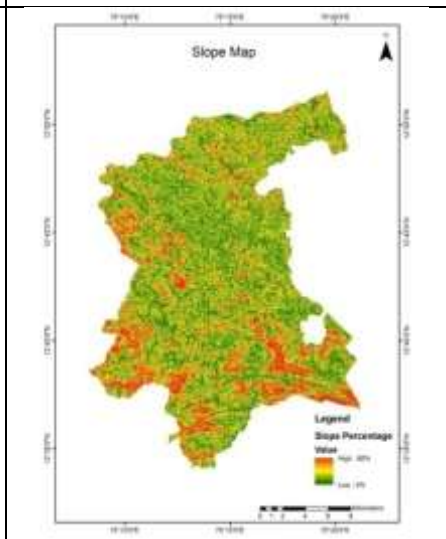
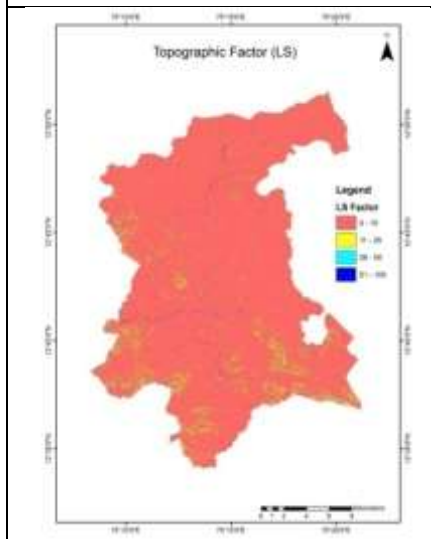
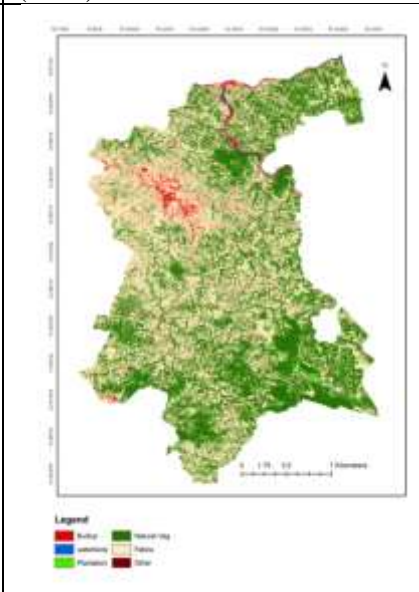
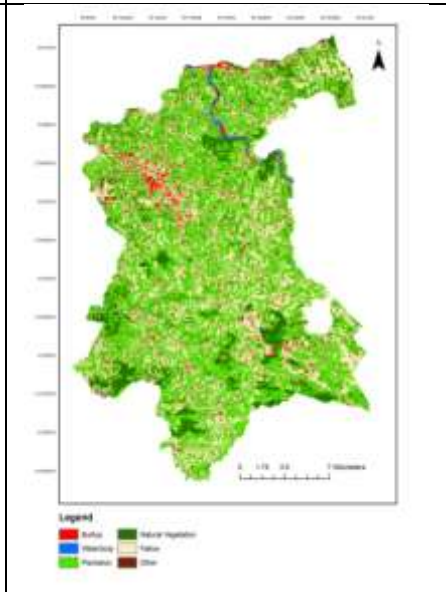
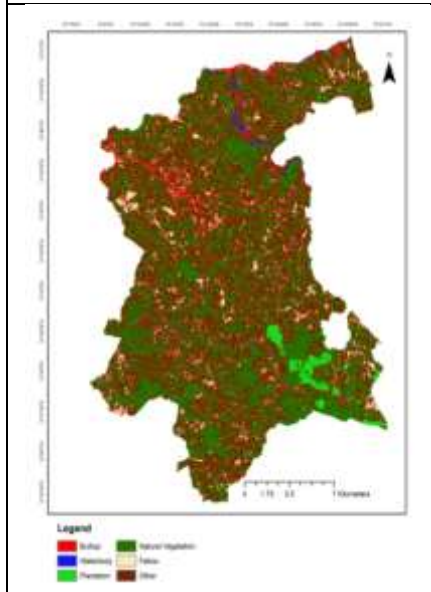
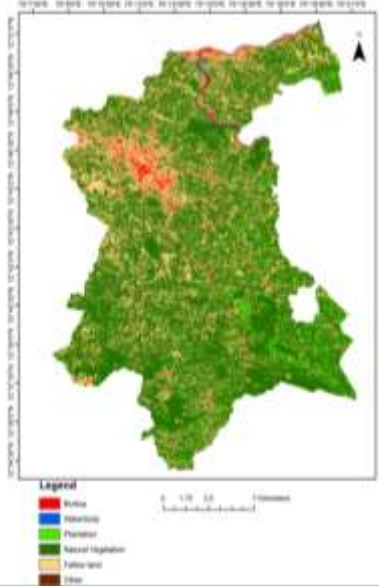
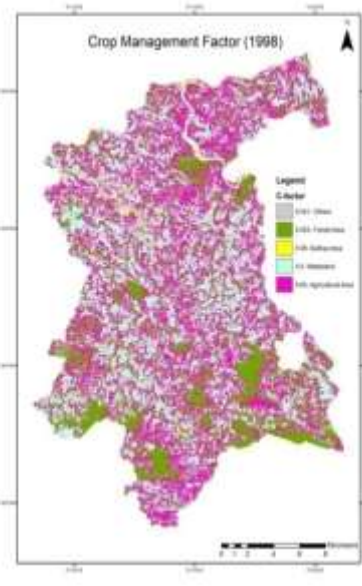
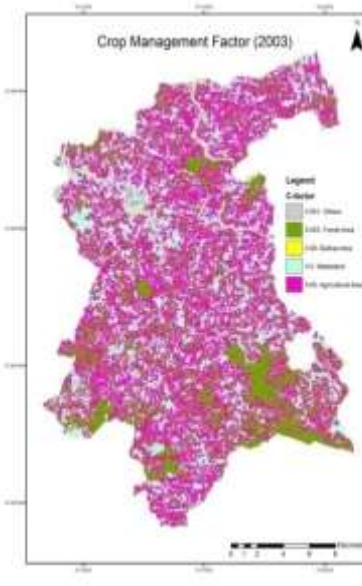


Fig 15: Topographic factor map

Fig 16: Slope Map

Fig 17: LULC Classification (1998)



<p>Fig 18: LULC Classification (2003)</p>	<p>Fig 19: LULC Classification (2008)</p>	<p>Fig 20: LULC Classification (2013)</p>
		
<p>Fig 21: LULC Classification (2019)</p>	<p>Fig 22: Crop management factor (1998)</p>	<p>Fig 23: Crop management factor (2003)</p>

3.2. Soil Erodibility Factor

The erodibility factor of soil is the susceptibility of a given soil type and location to the erosive forces of precipitation and runoff (K). It is believed that soil erodibility is influenced by factors such as soil texture, organic matter content, soil structure, and permeability. Values of soil erodibility close to 1 indicate a soil that is easily eroded, while values closer to zero, indicate a soil that is resistant to erosion.

The data used for this comes from open land maps, which can be found at <https://www.openlandmap.org/>. The resolution of these maps is only 250 metres. K is determined by comparing two maps: one showing the distribution of soil organic carbon at the soil's surface (depth 0m) and another showing the distribution of soil texture classes at the same level. The value of K can be determined by solving eq.(2).

$$K = 27.66 \times m^{1.14} \times 10^{-8} \times (12 - a) + 0.0043 \times (b - 2) + 0.0033 \times (c - 3) \tag{2}$$

Here m=(% silt+% very fine sand) x (100-(% clay)), organic material percentage c = profile permeability code; 1 = quick, 2 = moderate to rapid, 3 = moderate, 4 = slow, 5 = sluggish, and 6 = extremely slow, b = structure code; (1) = very structured or particulate, (2) = somewhat structured, (3) = slightly structured, and (4) = solid

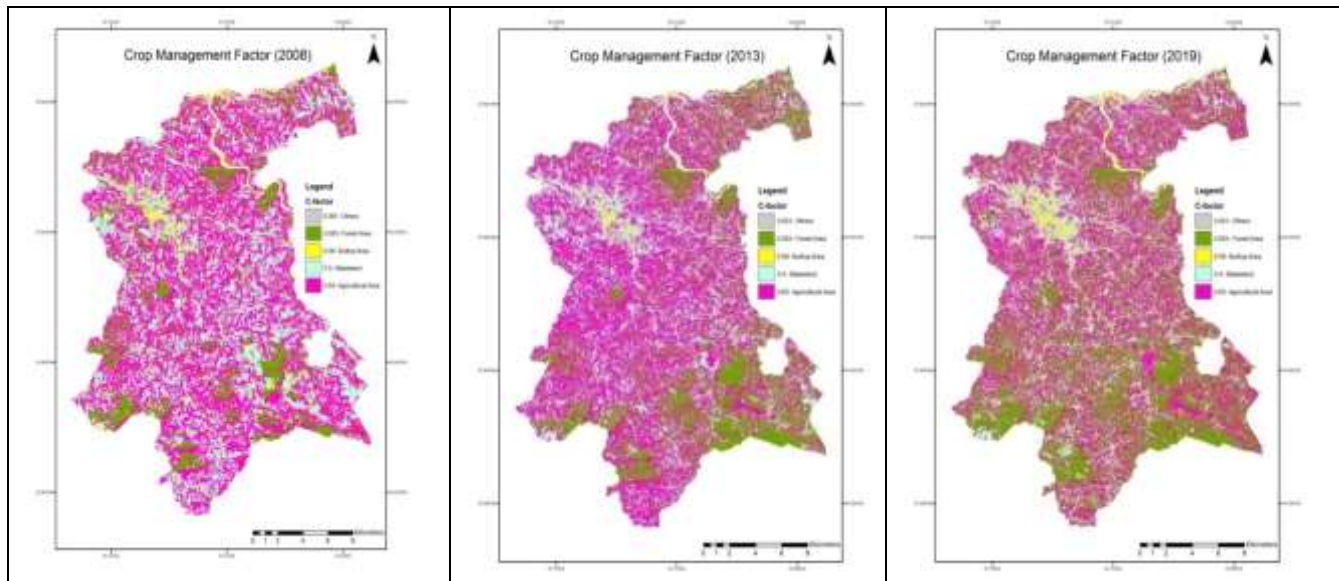


Fig 24: Crop management factor (2008)

Fig 25: Crop management factor (2013)

Fig 26: Crop management factor (2019)

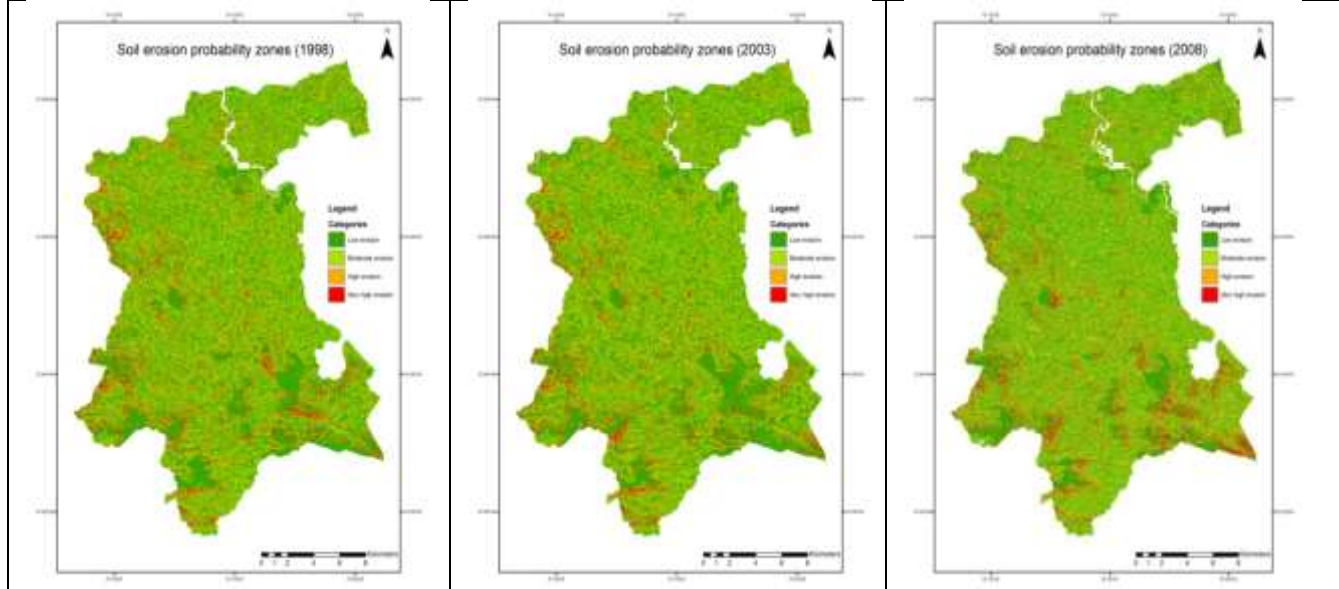


Fig 27: Soil erosion probability zones(1998)

Fig 28: Soil erosion probability zones(2003)

Fig 29: Soil erosion probability zones(2008)

3.3. Topographic Factor

The LS factor summarises topography's effects on erosion by combining slope length and slope angle. S-factor quantifies slope steepness and L-factor slope length. L is the horizontal distance between an upslope slope segment and a downslope deposition. Length and slope per unit area increase runoff and flow velocity, causing soil erosion. LS was calculated using 30 m SRTM DEM. The topographic factor (LS) is determined using eq. 3.

$$LS = \left[\frac{Q_{aM}}{22.13} \right]^y \times (0.065 + 0.045 \times S_g + 0.0065 \times S_g^2) \quad (3)$$

Here, where LS = Topographical factor; Q_a = Flow Accumulation grid; S_g- Grid slope in percentage; M Grid size (x * y), y dimensionless exponent that assumes the value of 0.2 to 0.5.

3.4. LULC Classification

Image categorization algorithms can be unsupervised or supervised. Supervised classification assumes a user may select training sites in an image that represent specific classes and then command image processing tools to generalize these classifications to the

remainder of the image. User expertise determines training sites (also known as testing sets or input classes). In addition, the user can set a similarity threshold below which no additional pixels will be grouped. The spectral properties of the training area are often used as a starting point for establishing these boundaries, plus or minus a given increment.

Maximum likelihood classification assesses the likelihood that a pixel belongs to a specific class by assuming each class's statistics are normally distributed. Unless a threshold is set, all pixels are labelled. Pixels are labelled with the most likely category (that is, the maximum likelihood). Pixels with a low likelihood are not classified.

Satellite imagery from 1998, 2003, 2008, 2013, and 2019 are used to create the LULC categorization. Built-up areas, water, fallow land, natural vegetation, plantations, and other land types have all been assigned distinct spectral groups based on a priori information. To ensure that the training samples for the aforementioned classes are representative of the location under review, adequate numbers of samples are gathered. A classification procedure with an accuracy of 90% or above is generated using the maximum likelihood technique. Crop management elements from the RUSLE guidebook are also assigned to these groups. The LULC classification of the research region for the study period is shown in Figs. 17 to 21 and in Table. 1.

Table 1: Area of LULC Classification

Area in sq km	1998	2003	2008	2013	2019
Others	5.93	9.11	26.90	5.02	10.67
Forest	90.51	93.59	57.49	97.38	141.37
Built Up	6.98	5.12	7.26	8.24	12.25
Wasteland	161.46	123.47	127.06	111.99	90.25
Agriculture	152.66	186.63	199.14	194.65	163.45

3.5. Land Cover and Management Factor

Aspects of land use and management C plays a crucial role by dispersing the effect of raindrops on the soil surface, thereby capturing changes in soil loss between vegetated and bare areas. The C factor ranges from 1 to 0; its value changes as soil erosion control measures employing plant cover and agricultural management techniques. The C factor is now computed using land use maps produced from supervised classification of satellite imagery. A bare reference plot with a C factor of 1 is used to get the soil loss ratio, which is then used to derive the C factor for each land use (Table. 2).

Table 2: C factor values for LULC classes

Sl. No.	Class Name	C factor
1	Water	0
2	Built-up	0.09
3	Agricultural area	0.63
4	Others	0.001
5	Waste land	0.50
6	Forest area	0.003

3.6. Support Practice Factor

The role of supportive practices that effect surface management practices which prevent soil erosion are expressed as P. This category includes techniques including terracing, strip cropping, and contour ploughing. P factors can take on values between 0 and 1, with 0 indicating the highest possible level of conservation practise efficacy and 1 signifying the absence of any such practises or measures. There is no significant supportinve management practices in the study area so the value of P is taken as 1.

4. Results and Discussions

4.1. Soil erosion

RUSLE (Wischmeier and Smith, 1978) calculates yearly field slope erosion using eq. (4).

$$A=RKLSCP \quad (4)$$

Here A = calculated spatial and temporal average soil loss per unit area, in K and R units. In practice, these units are chosen such that A is expressed in t/ ha/yr.

4.2. Soil Erosion Probability Zones

RUSLE simulations generate temporal soil erosion maps. According to Table 3, these are classified as low, moderate, high, and very high erosion probability zones.

Table 3: Categories of Soil Erosion

Erosion probability zone	Value (T/Ha/Year)
Low Erosion	0-100
Moderate Erosion	101-1000
High Erosion	1001-5000
Very High Erosion	>5001

Figures 27 to 31, display comparable probability zones for the study period. One reason for this is the trend towards reclaiming formerly unproductive land for agricultural use. Differences in C factor between agricultural land (0.63 in this case) and wasteland (0.5) are not statistically significant when compared to the other LULC groups. In 2008, the forested area shrank by 2.9%. The outcome is an increase of 2.4% in moderate soil erosion zones and a decrease of 3.5% in low soil erosion zones.

In 2013, there was no notable expansion of farmland but, Transformation of wastelands into forest is observed. Both the amount of forested land and the amount of waste land have dropped by 3.8%. As a result of the recent downpour, however, the percentage of land affected by high and very high soil erosion is risen to 3.8% and 2.8%, respectively. Both high and very high soil erosion zones have decreased since 2013, despite the fact that the average annual rainfall in both years is the same as it is in 2019. This is because forest coverage expanded by 2.9%, while waste land decreased by 5.1%.

4.3. Temporal soil loss

Summary of soil loss by erosion risk zone is shown in Table 4. In the years after 1998–2003 drought, soil loss dropped by 920 tonnes annually. Between 2003 and 2008, annual soil loss averaged 3,833 metric tonnes. Rainfall increase and deforestation are to be blamed for this phenomenon. It is important to remember that all erosion likelihood zones experience the same amount of soil loss.

Heavy rains in the year 2013 created flash floods over the region, resulting in the loss of 68,737 metric tonnes of soil. Very high erosion probability zone accounts for 61.3% of total soil loss (42,177 tons/year) and covers 6.69 percent of the research area. In most cases, these regions are located beside rivers (nearby streams). In 2019, the rate of soil loss fell to 37,022 tonnes annually, largely as a result of increased forest cover. The graphical representation of the soil loss over the time period is shown in Fig.34 and Table.4.

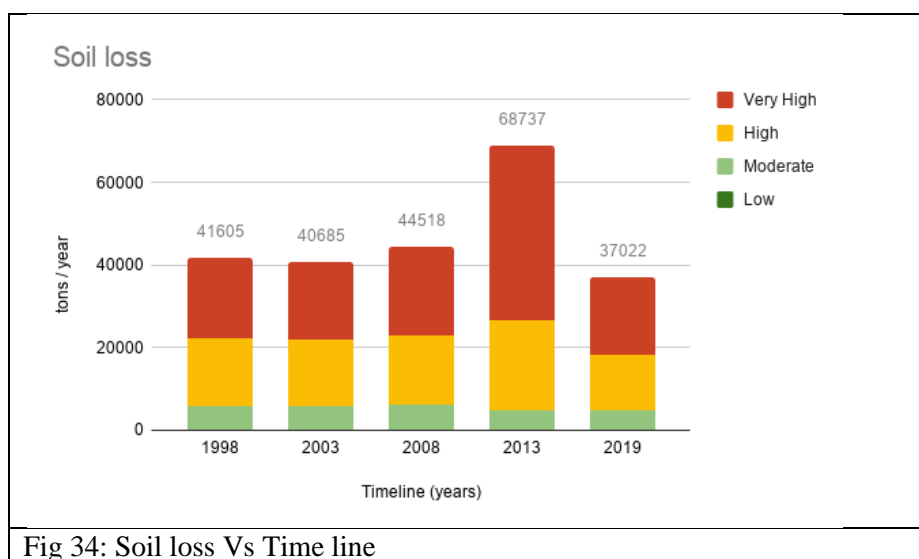


Fig 34: Soil loss Vs Time line

Table 4: Soil loss and area

Year Zone	1998		2003		2008		2013		2019	
	soil loss	% area	soil loss	% area	soil loss	% area	soil loss	% area	soil loss	% area
Low	134	53.65	129	54.36	121	50.88	123	52.2	173	61.9
Moderate	5672	26	5615	25.8	5945	28.2	4809	20.37	4550	21.17
High	16588	16.89	16280	16.51	16888	17.03	21628	20.75	13676	13.68
Very High	19211	3.46	18661	3.34	21564	3.89	42177	6.69	18623	3.25
Total	41605		40685		44518		68737		37022	

5. CONCLUSIONS

Amount of soil erosion is expected to rise as industrialization and urbanization convert forests and wetlands into farmland and human settlements in the study area. This shift in land use and land cover has affected hydrological parameters such as soil erosion, sediment deposition in the study area.

The data for years 1998, 2003, and 2008 indicates development of similar likelihood zones. This is due to conversion of unused land into agricultural land. The difference in C factor for agricultural land (0.63) and wasteland (0.5) is not significant compared to the other LULC classes. In the time period 1998 to 2003, soil loss dropped by 920 tonnes annually due to decreases in the rainfall. Between 2003 and 2008, annual soil loss averaged 3,833 metric tonnes which is the result of increase in the rainfall and deforestation.

It is important to remember that all erosion probability zones experience the same amount of soil loss. Heavy rains in the year 2013 created flash floods over the region, resulting in the loss of 68,737 metric tonnes of soil. Very high erosion probability zone accounts for 61.3% of total soil loss (42,177 tons/year) and covers 6.69 percent of the research area. In most cases, these regions are located beside rivers (nearby streams). In 2019, the rate of soil loss fell to 37,022 tonnes annually, largely as a result of increased forest cover.

The erosion susceptibility map which are developed as a result of this research study is a useful resource for stakeholders, decision-makers, and government officials involved in the planning of erosion catastrophe management. The maps provides information for emergency erosion control activities with the goal of reducing the negative effects of erosion in Puttur taluk.

Data Availability

The raw data used to support the findings of this study are available from the corresponding author upon request.

Acknowledgements

We would like to express our gratitude to everyone who helped us throughout the process of completing this research work, including our teachers, students, families, reviewers and friends. This work was supported by VGST, Government of Karnataka.

Funding

This research was done as part of the grant received by the , “ VISION GROUP ON SCIENCE AND TECHNOLOGY (VGST), Department of Information Technology, Biotechnology & Science & Technology Karnataka Government, is acknowledged by the authors for providing research facilities.

Contributions

Prasad Pujar: conceptualization, data curation, formal data analysis, visualization, writing—original draft and editing. Sowmya N J and Sandeep J Nayak: conceptualization, investigation, validation, writing—review and editing, and supervision. Sanjay Shekhar N C: writing, review and editing.

Ethics declarations

Competing interests

The authors declare no competing interests.

REFERENCES

- Borrelli, P., Alewell, C., Alvarez, P., Anache, J. A. A., Baartman, J., Ballabio, C., ... & Panagos, P. (2021). Soil erosion modelling: A global review and statistical analysis. *Science of the total environment*, 780, 146494.
- Chauhan, H. B., & Nayak, S. (2005). Land use/land cover changes near Hazira Region, Gujarat using remote sensing satellite data. *Journal of the Indian society of Remote Sensing*, 33, 413-420.
- Devia, G. K., Ganasri, B. P., & Dwarakish, G. S. (2015). A review on hydrological models. *Aquatic procedia*, 4, 1001-1007.
- Ganasri, B. P., & Ramesh, H. (2016). Assessment of soil erosion by RUSLE model using remote sensing and GIS-A case study of Nethravathi Basin. *Geoscience Frontiers*, 7(6), 953-961.
- Gumageri, N., & Dwarakish, G. S. (2011). Shoreline changes along the Mangalore coast, West coast of India. *Int J Earth Sci Eng*, 4(03), 63-70.
- Hütt, C., Koppe, W., Miao, Y., & Bareth, G. (2016). Best accuracy land use/land cover (LULC) classification to derive crop types using multitemporal, multisensor, and multi-polarization SAR satellite images. *Remote sensing*, 8(8), 684.
- Jones, K. B., Neale, A. C., Nash, M. S., Van Remortel, R. D., Wickham, J. D., Riitters, K. H., & O'Neill, R. V. (2001). Predicting nutrient and sediment loadings to streams from landscape metrics: a multiple watershed study from the United States Mid-Atlantic Region. *Landscape Ecology*, 16, 301-312.
- LemlemTadesse ,Suryabhagavank.V., G.Sridhar , Gizachew L. (2017), "Land use and land cover changes and Soil erosion in Yezat Watershed, North Western Ethiopia", *International Soil and Water Conservation Research*, Issue - 5, pp.85–94.
- Lin, W., Zhang, L., Du, D., Yang, L., Lin, H., Zhang, Y., & Li, J. (2009). Quantification of land use/land cover changes in Pearl River Delta and its impact on regional climate in summer using numerical modeling. *Regional Environmental Change*, 9, 75-82.
- Liu, X., Ren, L., Yuan, F., Singh, V. P., Fang, X., Yu, Z., & Zhang, W. (2009). Quantifying the effect of land use and land cover changes on green water and blue water in northern part of China. *Hydrology and Earth System Sciences*, 13(6), 735-747.
- Niehoff, D., Fritsch, U., & Bronstert, A. (2002). Land-use impacts on storm-runoff generation: scenarios of land-use change and simulation of hydrological response in a meso-scale catchment in SW-Germany. *Journal of hydrology*, 267(1-2), 80-93.
- Patel, S. K., Verma, P., & Shankar Singh, G. (2019). Agricultural growth and land use land cover change in peri-urban India. *Environmental monitoring and assessment*, 191, 1-17.
- Patz, J. A., Campbell-Lendrum, D., Holloway, T., & Foley, J. A. (2005). Impact of regional climate change on human health. *Nature*, 438(7066), 310-317.
- Qian Cao, Deyong Yu, Matei Georgescu, Zhe Han and Jianguo Wu (2015)," Impacts of land use and land cover change on regional climate: A case study in the agro-pastoral transitional zone of China", *Environmental Research Letters Publishing Ltd:Volume- 10* , pp. 1-12.

- Verburg, P. H. (2006). Simulating feedbacks in land use and land cover change models. *Landscape Ecology*, 21, 1171-1183.
- Verburg, P. H., Kok, K., Pontius Jr, R. G., & Veldkamp, A. (2006). Modeling land-use and land-cover change. In *Land-use and land-cover change: local processes and global impacts* (pp. 117-135). Berlin, Heidelberg: Springer Berlin Heidelberg.
- Wang, Q., Guan, Q., Lin, J., Luo, H., Tan, Z., & Ma, Y. (2021). Simulating land use/land cover change in an arid region with the coupling models. *Ecological Indicators*, 122, 107231.
- Wijesekara, G. N., Gupta, A., Valeo, C., Hasbani, J. G., Qiao, Y., Delaney, P., & Marceau, D. J. (2012). Assessing the impact of future land-use changes on hydrological processes in the Elbow River watershed in southern Alberta, Canada. *Journal of hydrology*, 412, 220-232.
- Wischmeier, W. H., & Smith, D. D. (1978). *Predicting rainfall erosion losses: a guide to conservation planning* (No. 537). Department of Agriculture, Science and Education Administration.
- Yuechen, L. I. (2008). Land cover dynamic changes in northern China. *J. Geogr. Sci*, 18, 85-94.